The Cryosphere Discuss., 2, 811–841, 2008
www.the-cryosphere-discuss.net/2/811/2008/

The Cryosphere Discussions

The Cryosphere Discussions is the access reviewed discussion forum of *The Cryosphere*

A new 1 km digital elevation model of the Antarctic derived from combined satellite radar and laser data – Part 1: Data and methods

J. L. Bamber[1,2], **J. L. Gomez-Dans**[1,*], **and J. A. Griggs**[2]

[1]Centre for Polar Observations and Modelling, School of Geographical Sciences, University of Bristol, UK
[2]Bristol Glaciology Centre, School of Geographical Sciences, University of Bristol, UK
[*]now at: Environmental Monitoring Group, Department of Geography, King's College London, UK and Remote Sensing Unit, Department of Geography, University College London, UK

Received: 18 September 2008 – Accepted: 26 September 2008 – Published: 25 November 2008

Correspondence to: J. L. Bamber (j.bamber@bristol.ac)

Published by Copernicus Publications on behalf of the European Geosciences Union.

Abstract

Digital elevation models (DEMs) of Antarctica have been derived, previously, from satellite radar altimetry (SRA) and limited terrestrial data. Near the ice sheet margins and in other areas of steep relief the SRA data tend to have relatively poor coverage and accuracy. To remedy this and to extend the coverage beyond the latitudinal limit of the SRA missions (81.5° S) we have combined laser altimeter measurements from the Geosciences Laser Altimeter System onboard ICESat with SRA data from the geodetic phase of the ERS-1 satellite mission. The former provide decimetre vertical accuracy but with poor spatial coverage. The latter have excellent spatial coverage but a poorer vertical accuracy. By combining the radar and laser data using an optimal approach we have maximised the vertical accuracy and spatial resolution of the DEM and minimised the number of grid cells with an interpolated elevation estimate. We assessed the optimum resolution for producing a DEM based on a trade-off between resolution and interpolated cells, which was found to be 1 km. This resulted in just under 35% of grid cells having an interpolated value. The accuracy of the final DEM was assessed using a suite of independent airborne altimeter data and used to produce an error map. The RMS error in the new DEM was found to be roughly half that of the best previous 5 km resolution, SRA-derived DEM, with marked improvements in the steeper marginal and mountainous areas and between 81.5 and 86° S. The DEM contains a wealth of information related to ice flow. This is particularly apparent for the two largest ice shelves – the Filchner-Ronne and Ross – where the surface expression of flow of ice streams and outlet glaciers can be traced from the grounding line to the calving front. The surface expression of subglacial lakes and other basal features are also illustrated. We also use the DEM to derive new estimates of balance velocities and ice divide locations.

TCD

2, 811–841, 2008

1 Introduction

Surface topography is an important data set for a wide range of applications from fieldwork planning to numerical modelling studies. It can, for example, be used to validate the ability of a model to reproduce the present-day geometry of the ice sheet or as an input boundary condition for modelling or combined with other data to estimate steady-state velocities and ice thickness (Bamber et al., 2000; Budd and Warner, 1996; Warner and Budd, 2000). Estimates of the mass balance of Antarctica using a mass budget approach are critically dependent on accurate surface topography for estimating i) drainage basin areas and ii) ice thickness close to the grounding line (Joughin and Bamber, 2005; Rignot and Thomas, 2002; Rignot et al., 2008) as direct measurements of ice thickness are sparse. A recent study of the accuracy of existing, published DEMs of Antarctica, found that large errors (in excess of hundreds of metres) were ubiquitous in areas of higher surface slope such as near the margins of the ice sheet, in mountainous terrain such as the Transantarctic Mountains and also beyond the latitudinal limit of satellite radar altimeter measurements (Bamber and Gomez-Dans, 2005).

As a consequence of the limitations in the existing DEMs and the availability of a source of high accuracy elevation data for many of the areas that are "problematic" for SRAs, we have produced a new DEM of the Antarctic continent. We have combined the high-accuracy, but relatively low spatial resolution, laser altimeter measurements from the Geoscience Laser Altimeter System, GLAS, onboard the ICESat satellite, with radar altimeter data from the geodetic phase of the ERS-1 satellite, which provide high spatial sampling but lower vertical accuracy. The result is a DEM, where the number of interpolated grid points has been minimised while improving the accuracy of the topography for areas of high relief and south of 81.5° latitude. Stereo-photogrammetric and cartographic data have not been used in this study although they may be able to improve the accuracy of the DEM in high-relief regions such as the Transantarctic Mountains (Liu et al., 1999).

TCD
2, 811–841, 2008

2 Data sets and processing

In March 1995 ERS-1 was placed in two long repeat cycles of 168 days. The two phases were offset from each other so that they were equivalent to a single 336 day cycle, providing 8.3 km across-track spacing at the equator. This reduces to about 4 km at 60° latitude and 2 km at 70°. The along-track spacing of each altimeter height measurement is 335 m. The total number of data points, after filtering, over the ice sheet was about 40 million (Bamber and Bindschadler, 1997). The data reduction methodology has been described, in detail, elsewhere (Bamber, 1994; Bamber and Huybrechts, 1996) and this is the same data set that was used to produce an earlier 5 km posting DEM of Antarctica (Bamber and Bindschadler, 1997).

We have combined the ERS-1 data with all the available, reliable GLAS data, as listed in Table 1. GLAS has an along track spacing of 170 m and an across-track spacing of about 20 km at 70° S. The data product used here was the level 2 Antarctic and Greenland Ice Sheet Altimetry Data product (GLA12) and all data used were release version 428 (Zwally et al., 2007). The data were extracted using the software provided by the National Snow and Ice Data center (NSIDC) and transformed from the Topex/Poseidon ellipsoid to the WGS84 ellipsoid for consistency with the ERS-1 data and the geoid model applied. Corrections were also applied to account for saturation of the laser over the ice sheet as recommended by the NSIDC.

Geophysical quality assurance filters were used to remove those returns which may contain residual cloud or other artefacts that affect the elevation estimate. The geophysical filters used were:

1. Attitude control classified as good
2. Only 1 waveform detected
3. Reflectivity of surface greater than 10%
4. Gain less than 200

TCD
2, 811–841, 2008

5. Variance of waveform from Gaussian less than 0.03 V

These filters combined, removed 7.7% of the data (Table 2).

The data were gridded with 5 km spacing and a 3 standard deviation filter was applied to remove additional elevation outliers. Visual inspection indicated that a small number of anomalous ERS and GLAS data remained and these were removed in a final filtering step. This was achieved by using an preliminary version of the 1 km DEM (Bamber and Gomez-Dans, 2005) and removing points where the difference was >(11.5*slope angle) for slopes between 0.1° and 1°. These values were chosen based on the standard deviation of differences between GLAS and ERS data as a function of surface slope derived in an earlier study (Bamber and Gomez-Dans, 2005). Data were only filtered in this step if they originate from an area where the surface slope was less 1°. In areas of higher slope, individual returns may be expected to have large departures from the average surface height in the grid box and so such a filter is inappropriate. Also at these higher surface slopes, there are relatively few data points in the comparison between GLAS and ERS. Surface slopes were determined with a 2 km spatial resolution from the "first guess" DEM. This final quality assurance filter removed a further 4% of the original data. A GLAS roughness filter, used in the earlier study (Bamber and Gomez-Dans, 2005) was not applied here. This filter used a roughness estimate derived from the GLAS waveforms. The most recent data releases no longer contain this variable due to errors in the way it was calculated. The pattern of surface slopes over the ice sheet, as determined from the final DEM, is shown in Fig. 1 to indicate the regions affected by this filter and the range of surface slopes over the continent.

2.1 ERS data pre-processing

The ERS data used are the same as those used to derive a 5 km Antarctic DEM in the 1990s (Bamber and Bindschadler, 1997). The data have been retracked, slope-corrected and filtered, as described elsewhere (Bamber, 1994; Bamber and Bindschadler, 1997). These data were shown to suffer a roughness-dependent surface

bias, which was believed to be due to the fact that the SRA does not sample kilometre scale surface roughness uniformly (Bamber, 1994; Bamber et al., 1998; Bamber and Gomez-Dans, 2005). Instead the peaks of undulations are oversampled compared to the troughs, causing a positive bias in the observed elevations, which increases with the amplitude of the undulations. The bias was removed by calculating the difference between the ERS-1 and GLAS data as a function of surface roughness over a length scale of 5 km. Surface roughness was determined from the standard deviation of the surface slope of a "first guess" DEM for a 5×5 grid centred on the cell in question. The bias, calculated as a function of roughness, binned with 0.01° intervals is shown in figure 2. Up to a roughness of ~0.15°, there is a near-linear increase in bias from zero to 16 m. Beyond this point the relationship breaks down. Figure 3 shows the spatial pattern of the correction applied to the ERS data based on the relationship shown in Fig. 2 up to a roughness of 0.25°. The unshaded areas over the ice sheet in Fig. 3 are regions where the roughness either exceeded 0.25° or where no ERS data were present. This is generally in areas of high relief where the increased roughness and the variable surface gradients caused the ERS-1 radar altimeter to lose lock of the surface return. It should be noted that the roughness estimate described above correlates closely with regional surface slope (Fig. 1) except in areas where the second derivative of the surface is small, such as on the ice rises and islands on the Ross and Filchner Ronne ice shelves (see inset in Fig. 3). These areas are "smooth" over kilometre length-scales while possessing a non-negligible regional slope (Fig. 1). It was largely for this reason that, here, we determined the bias as a function of roughness (Griggs and Bamber, 2008) as opposed to surface slope as was done in earlier studies (Bamber et al., 1998; Bamber and Gomez-Dans, 2005).

2.2 Time stamp and data weighting

The ERS data are not contemporaneous with the GLAS observations and so a correction for surface elevation changes between the acquisition period of the ERS data (1994–1995) and the GLAS data (2003–2006) was applied. Here, we used annual

elevation change estimates derived from ERS radar altimetry between 1992 and 2003 (Davis et al., 2005). A correction was only applied in regions where the height change over the entire period was more than 1m as this was assumed to be the likely cumulative error in the measurements based on an ~10 cm/yr detection limit.

A number of previous studies have shown that the RMS error of SRA over the ice sheets degrades with increasing regional slope (Bamber et al., 1998; Bamber and Gomez-Dans, 2005; Brenner et al., 2007). The SRA data were, therefore, weighted according to an estimate of their accuracy as a function of surface slope. The weights were calculated using the equation below, which was derived from a degree-two polynomial fit to the standard deviation of the difference between GLAS and ERS data as a function of surface slope.

$$\text{weight} = \begin{cases} \dfrac{2.35255}{2.35255 + 19.3115 * \text{slope} + 16.1766 * \text{slope}^2} & \text{for slope angles} < 1^\circ \\ \dfrac{1}{50} & \text{for slope angles} \geq 1^\circ \end{cases}$$

2.3 Choice of DEM resolution

An optimal DEM resolution is desirable, which is a trade-off between minimizing the number of interpolated points, while maximising the spatial detail in the original data. The metric used to determine the optimum resolution here was the ratio between the number of grid cells containing observations against those that did not (i.e. grid cells where the value is interpolated). For convenience, we have called this the interpolation ratio. The coverage of the two altimeters used in this study is latitude dependent, increasing toward the latitudinal limit of the satellite orbits of 81.5° and 86° for ERS-1 and ICESat respectively (Fig. 4). We examined the interpolation ratio for three latitudinal bands: 70–75, 75–80 and 80–85° S. The first band is largely populated, numerically, by ERS data, the middle band is a mixture of the two while the last band is dominated by ICESat data. The number of observations, however, does not necessarily reflect the "importance" of ERS data compared to ICESat because, in areas of higher slope in particular, the ERS data may be heavily down-weighted. Thus, for example, where the

slope is greater than 1°, 50 SRA observations have the same weight as a single GLAS observation. Nonetheless, Fig. 4 illustrates some important points about the variability in spatial sampling by ERS and GLAS, as a function of latitude and surface slope. The white bands at ~81 and ~86° S indicate the latitudinal limits of the two satellites, where coverage is dense and spatial sampling high. The light-coloured lines crossing the continent indicate ICESat tracks where, locally, the sampling is high because we have used multiple repeat tracks. Between these lines are areas of blue to green and yellow, which reflect grid cells where only ERS data are present. This can be more clearly seen in Fig. 4b and c. The latter (the Amery Ice Shelf) covers an area relatively far north at around 70° S where the across track spacing of ICESat is evidently course and where the majority of the grid cells are populated by ERS data only. In the area just upstream of the grounding line of the ice shelf is a band of black, where no data are present, most probably due to the high relief in this area and the filters applied to the ERS data described earlier. The dense coverage provided by ERS-1 over the two largest ice shelves is illustrated in Fig. 4b and is due to the low relief and proximity to the latitudinal limit of the satellite. Figure 4 demonstrates the importance of the ERS-1 data for providing observations between the ICESat tracks, particularly for latitudes north of about 80°, where the across-track spacing of ICESat is around 15 km.

The interpolation ratios were calculated using the number of valid data points within each latitude band, which were binned into cells with spacings between 500 and 5000 m. Figure 5 shows the results of this analysis. For a cell size of 1 km, the percentage of interpolated points (i.e. those where no satellite data fall within the grid cell) is between 20 and 40% depending on the latitude band. At resolutions smaller than this, the percentage rapidly increases. We believe, therefore, that a DEM with 1 km postings provides a realistic representation of the true resolution of the input data at the continental scale. Using this value, resulted in just under 35% of grid cells having an interpolated value or, put another way, 65% of grid cells contained measured elevation estimates. A variable resolution DEM or regional models at higher resolution could be considered, particularly in areas close to latitudes of 81.5 and 86° S.

2.4 Data gridding and interpolation

Data were first re-sampled onto a quasi-regular 1km grid by calculating the mean x, y and z values for each cluster of satellite data falling within a grid cell. The mean z estimates were weighted values of the combined ERS and GLAS data. The weights for GLAS data were 1.0 and for the ERS data were inversely proportional to the variance of the difference between ERS and GLAS as a function of surface slope, as discussed earlier. A land/ocean mask was applied to the quasi regular grid so that data over ocean/sea ice were not included in the interpolation and did not create biases at the ice edge. The mask defining the coastline was created using version 5 of the Antarctic Digital Database (ADD consortium, 2006) which has a variable resolution of between 5 m and greater than 5 km. The data were then interpolated onto a regular 1 km polar stereographic grid with a standard parallel of 71° S, using a tension spline approach. This interpolation technique fits a semi-rigid membrane to the set of points from the quasi-regular grid. The rigidity of the membrane can be controlled and may vary between that representing a stiff steel plate with a minimum curvature solution and a rubber sheet resulting in mounts and pits due to the variation of individual points. The tension parameter changes the scale at which a single point affects its neighbours. A measure of flexibility can also be given to each vertical position in the surface. This means that the interpolated surface need not pass exactly through each point but can deviate from it by a given value. The open source software package GRASS was used for the interpolation. Through trial and error, a tension of 28 and smoothing parameter of 11 was found to be most effective. South of 86°, ADD cartographic data was merged with the DEM by weighting the two datasets using Hermite basis functions over a distance of 40 km at the southern limit of the satellite dataset.

3 Results

The complete DEM is shown in Fig. 6 and illustrates the large-scale topographic features such as ice divides, the ice shelves and the region lacking satellite coverage south of a latitude of 86°. Also shown are the location of ice divides obtained from the DEM and used in a mass budget study of the ice sheet to separate flow between drainage basins (Rignot et al., 2008).

It is not possible to see the full resolution and detailed topography at a continental scale. Figure 7 illustrates the finer-scale (both horizontal and vertical) topography present in the DEM for the Filchner-Ronne Ice Shelf. The red crosses are estimates of the location of the limit of flexure of the grounding zone obtained from repeat-track analysis of GLAS data (Fricker and Padman, 2006). There is good qualitative agreement between these points and the limit of floating ice based on the break in slope as identified from the DEM. Flow stripes, traceable from the grounding line to ice front are clearly visible and are associated with ice stream flow into the ice shelf and around grounded "obstacles" such as Berkner Island. Their amplitude varies between around 50 cm and 3 m and they have a width of a few kilometres, which is clearly resolved in the DEM (Fig. 8). Not surprisingly, the ICESat-only DEM, although gridded at 500 m, does not capture all the flow-stripe, due to the relatively sparse across-track spacing of the satellite (c.f. Fig. 4). The surface expression of ICESat tracks can be seen running east-west across the ice shelf indicating a likely bias between the ERS and GLAS data. The bias is between 5 and 10 cm and is visible because of the small variation in elevation on the ice shelves. The bias is a similar magnitude to the cumulative elevation changes estimated from radar altimeter data (Zwally et al., 2005). These elevation changes were not available over the ice shelves and this may be the cause for the difference. It may also be partly due to errors in the tide models used to correct the satellite data. In this study, we used the tide correction provided with the GLA12 product for the GLAS data. As part of an ongoing study focusing specifically on the ice shelves in Antarctica, we are replacing this tide model with an improved version that

TCD
2, 811–841, 2008

has been validated specifically for the Southern Ocean (King and Padman, 2005).

The new DEM has been used in a number of applications already including inferring subglacial topography in East Antarctica (Le Brocq et al., 2008) and estimating grounding line fluxes for mass budget calculations (Joughin and Bamber, 2005; Rignot et al., 2008). It has also been used to re-calculate balance velocities. These are the depth-averaged velocity required to maintain the ice sheet in a state of mass balance and were estimated using an ERS-only DEM previously (Bamber et al., 2000). Here, we have combined the new DEM with the BEDMAP ice thickness data set (Lythe and Vaughan, 2001) and surface mass balance data from the output of a regional climate model (van de Berg et al., 2006). The result is shown in Fig. 10. The most significant differences in the spatial pattern of balance velocities compared to the previous result is for the region between 81.5 and 86° S. In particular the glaciers feeding the Ross Ice Shelf through the Transantarctic mountains and the ice streams along the Siple Coast have a somewhat different "structure". Differences here and further north, such as along the Amundsen Sea sector and feeding Getz Ice Shelf are also due to significant differences in the spatial pattern of accumulation produced by the regional climate model compared with the observationally-based data set used in the earlier analysis (van de Berg et al., 2005).

To investigate the impact of the new DEM on the delineation of ice divides we have compared those derived from the older, 5 km DEM derived from ERS-1 data, which were used in a reassessment of the mass balance of Antarctica (Vaughan et al., 1999) with those derived from the new DEM and used for a similar purpose (Rignot et al., 2008). The comparison is shown in Fig. 11. Not surprisingly, the agreement is good for the low-slope Antarctic plateau region up to the latitudinal limit of ERS-1 (green circle). Between this and the limit of ICESat (blue circle) there are differences in basin area as well as in the fidelity of the delineation process. The red ice divides (using the new DEM) separate the catchments for each ice stream feeding the Filchner Ronne and Ross ice shelves. This was not possible, within acceptable errors, with the earlier DEMs that did not incorporate ICESat data (Bamber and Bindschadler, 1997; Liu et

al., 1999). South of the blue circle, at 86° S there remains uncertainty over the catchment areas for Foundation and Support Force glacier based on, essentially the same terrestrial data.

3.1 Validation and error analysis

A suite of independent airborne elevation measurements have been used to assess the accuracy of the DEM as a function of surface slope, roughness and other parameters. These data were also used to produce an error map and the details are described in a companion paper (Griggs and Bamber, 2008). We summarize, therefore, the key points only. In comparison to the best (the one with the lowest RMS errors) of the two previously published DEMs derived primarily from SRA data (Bamber and Bindschadler, 1997; Liu et al., 1999) the RMS error has been reduced by about a factor two (Griggs and Bamber, 2008). The RMS differences are also less than a DEM derived solely from ICESat data (DiMarzio et al., 2008) but only by around 5–32% depending on the area considered. Uniquely for Antarctica, an error map has been derived based on the results of the validation analysis and a stepwise regression against the variables believed to be correlated with errors in the DEM.

4 Discussion

In an earlier study, GLAS data were used to assess the accuracy of two current DEMs of Antarctica (Bamber and Gomez-Dans, 2005). The accuracy was determined as a function of surface slope. One was found to have a monotonically increasing bias with slope with a value of around 10 m for a slope of 1°. The standard deviation for this DEM was ~45 m at the same angle and around 68 m for the other DEM. Comparison with a suite of independent validation data indicates that the random error in the new DEM, presented here, is around half that of the "better" of the two models assessed previously and that the bias is close to zero for all slopes (Griggs and Bamber,

2008). Between 81.5 and 86° S the improvement is greater still as the earlier DEMs were reliant on sparse, poor accuracy terrestrial data. The accuracy of topography in this region, prior to the launch of ICESat, was more like ±100 m (Bamber and Gomez-Dans, 2005). Not surprisingly, therefore, balance velocities estimated using the our new DEM differ significantly in terms of spatial pattern compared with an earlier estimate. The accuracy of the DEM south of 86° still remains an issue with no immediate solution evident. Balance velocities, and other variables sensitive to slope, such as ice divides, will continue to have a higher uncertainty south of 86°. Crucially, however, the satellite observations now cover the entirety of the grounding lines of all the ice shelves (Figs. 1 and 10). These data can, and have been used, therefore, to determine ice thickness close to the grounding line assuming hydrostatic equilibrium and taking account of firn density variations (Helsen et al., 2008; Rignot et al., 2008). As part of this work, elevations from the DEM along the grounding line of Ice Stream D were compared with airborne lidar data with an accuracy of <40 cm (Blankenship et al., 2001). The mean difference in elevation along the grounding line was 0.15 m±4.0 m. This implies a bias of around 1 m in ice thickness and random error of 35 m equivalent to ~5%. As mentioned previously, work is on-going focusing specifically on improving the accuracy of ice thickness measurements over all the ice shelves and, in particular, close to the grounding line. An improved tide model is being employed combined with GLAS data to constrain off-ranging errors in the ERS-1 data at the break in slope that occurs in this region. Figure 3 indicates that the bias in the ERS-1 data is small (5–10 cm) over the ice shelves but increases markedly inland of the grounding line. The bias (GLAS-ERS) is negative, indicating that the ERS-1 data are biased high. Not accounting for this bias could, therefore, result in an overestimating of ice thickness close to the grounding line. Additionally, it is evident that GLAS data alone are inadequate for determining grounding line elevations for all except those lying south of about 80° S (Fig. 4). Figure 12 shows the coverage of ICESat tracks over the Amery Ice Shelf, which lies at about 70° S in greater detail. The lighter (whiter) lines indicate the ICESat tracks. There are about fifteen covering the entirety of the grounding line (shown in

red) while the blue-green colours indicate ERS-1 data, which provide almost complete coverage at the grid spacing of 1 km used here. Inland of the grounding line is an ~20 km wide band shaded black, where the ERS-1 data are absent due to the steep relief and the filtering steps, described earlier, applied to the data.

5 Conclusions

We present a new digital elevation model of Antarctica with grid spacing of 1 km, chosen to balance the proportion of grid cells that contained an interpolated value while maximising the spatial resolution of the DEM. We undertook a careful and comprehensive filtering of both data sets using a range of geophysical and instrument-based tests to ensure that the effect of clouds and other artefacts were eliminated. An extensive suite of independent airborne laser and radar altimeter measurements was used to undertake a thorough analysis of the accuracy of the DEM. These data were also used to produce an error map (Griggs and Bamber, 2008). Random errors were found to be predominantly a function of surface slope and roughness, ranging between ~50 cm and 20 m for the RMS error and typical range of slopes/roughness over the ice sheet. This roughly halves the random error compared to an earlier DEM without the benefit of GLAS data (Bamber and Gomez-Dans, 2005). For the region between 81.5 and 86° S, the improvement in accuracy and resolution is larger still and has a marked effect on the spatial pattern of balance velocities and drainage basins derived using the new DEM.

Acknowledgements. This work was funded by UK NERC contract for the Centre for Polar Observations and Modelling and NERC grant NE/E004032/1.

References

ADD Consortium: Antarctic Digital Database, Version 5, Database, Manual and Bibliography, Scientific Committee on Antarctic Research, Cambridge, 2006.

Bamber, J. L.: Ice sheet altimeter processing scheme, Int. J. Remote Sens., 14, 925–938, doi:10.1080/01431169408954125, 1994.

Bamber, J. L. and Huybrechts, P.: Geometric boundary conditions for modelling the velocity field of the Antarctic ice sheet, Ann. Glaciol., 23, 364–373, 1996.

Bamber, J. L. and Bindschadler, R. A.: An improved elevation data set for climate and ice sheet modelling: Validation with satellite imagery, Ann. Glaciol., 25, 439–444, 1997.

Bamber, J. L., Ekholm, S., and Krabill, W. B.: The accuracy of satellite radar altimeter data over the Greenland ice sheet determined from airborne laser data, Geophys. Res. Lett., 25, 3177–3180, 1998.

Bamber, J. L., Vaughan, D. G., and Joughin, I.: Widespread complex flow in the interior of the Antarctic ice sheet, Science, 287, 1248–1250, 2000.

Bamber, J. L. and Gomez-Dans, J. L.: The accuracy of digital elevation models of the Antarctic continent, Earth Planet. Sc. Lett., 217, 516–523, 2005.

Blankenship, D. D., Morse, D. L., Finn, C. A., Bell, R. E., Peters, M. E., Kempf, S. D., Hodge, S. M., Studinger, M., Behrendt, J. C., and Brozena, J. M.: Geological controls on the initiation of rapid basal motion for the west Antarctic ice streams: A geophysical perspective including new airborne radar sounding and laser altimetry results, in: The west Antarctic ice sheet: Behavior and environment, edited by: Alley, R. B. and Bindschadler, R., American Geophysical Union, Washington DC, 105–122, 2001.

Brenner, A. C., DiMarzio, J. R., and Zwally, H. J.: Precision and accuracy of satellite radar and laser altimeter data over the continental ice sheets, IEEE T. Geosci. Remote, 45, 321–331, doi:310.1109/TGRS.2006.887172, 2007.

Budd, W. F. and Warner, R. C.: A computer scheme for rapid calculations of balance-flux distributions, Ann. Glaciol., 23, 21–27, 1996.

Davis, C. H., Li, Y., McConnell, J. R., Frey, M. M., and Hanna, E.: Snowfall-driven growth in east Antarctic ice sheet mitigates recent sea-level rise, Science, 308, L15502, doi:10.1126/science.1110662, 2005.

DiMarzio, J. P., Brenner, A. C., Schutz, B. E., Shuman, C. A., and Zwally, H. J.: GLAS/ICESat 500 m laser altimetry digital elevation model of Antarctica, Boulder, Colorado, USA, National

Snow and Ice Data Center, Digital Media, 2007.
Fricker, H. A. and Padman, L.: Ice shelf grounding zone structure from ICESat laser altimetry, Geophys. Res. Lett., 33, L15502, doi:10.1029/2006GL026907, 2006.
Griggs, J. A. and Bamber, J. L.: A new digital elevation model of Antarctica derived from combined radar and laser data – Part 2: Validation and error estimates, The Cryosphere, 2, 843-872, 2008.
Helsen, M. M., van den Broeke, M. R., van de Wal, R. S. W., van de Berg, W. J., van Meijgaard, E., Davis, C. H., Li, Y., and Goodwin, I.: Elevation changes in Antarctica mainly determined by accumulation variability, Science, 1153894, doi:10.1126/science.1153894, 2008.
Holt, J. W., Blankenship, D. D., Morse, D. L., Young, D. A., Peters, M. E., Kempf, S. D., Richter, T. G., Vaughan, D. G., and Corr, H. F. J.: New boundary conditions for the west Antarctic ice sheet: Subglacial topography of the Thwaites and Smith glacier catchments, Geophys. Res. Lett., 33, L09502, doi:10.1029/2005GL025561, 2006.
Joughin, I. and Bamber, J. L.: Thickening of the ice stream catchments feeding the Filchner-Ronne ice shelf, Antarctica, Geophy. Res. Lett., 32, L17503, doi:10.1029/2005GL023844, 2005.
King, M. A. and Padman, L.: Accuracy assessment of ocean tide models around Antarctica, Geophys. Res. Lett., 32, B08401, doi:10.1029/2004JB003390, 2005.
Le Brocq, A. M., Hubbard, A., Bentley, M. J., and Bamber, J. L.: Subglacial topography inferred from ice surface terrain analysis reveals a large un-surveyed basin below sea level in east Antarctica, Geophys. Res. Lett., 35, L16503, doi:10.1029/2008GL034728, 2008.
Liu, H. X., Jezek, K. C., and Li, B. Y.: Development of an Antarctic digital elevation model by integrating cartographic and remotely sensed data: A geographic information system based approach, J. Geophys. Res.-Sol. Ea., 104, 23 199–23 213, 1999.
Lythe, M. B. and Vaughan, D. G.: Bedmap: A new ice thickness and subglacial topographic model of Antarctica, J. Geophys. Res.-Sol. Ea., 106, 11 335–11 351, 2001.
Rignot, E. and Thomas, R. H.: Mass balance of polar ice sheets, Science, 297, 1502–1506, 2002.
Rignot, E., Bamber, J. L., van den Broeke, M. R., Davis, C., Li, Y., van de Berg, W. J., and van Meijgaard, E.: Recent Antarctic ice mass loss from radar interferometry and regional climate modelling, Nature Geosciences, 1, 106–110, doi:10.1038/ngeo102, 2008.
van de Berg, W. J., van den Broeke, M., and Reijmer, C. H.: Characteristics of the Antarctic surface mass balance (1958–2002) using a regional atmospheric climate model, Ann. Glaciol.,

41, 97–104, 2005.
van de Berg, W. J., van den Broeke, M. R., van Meijgaard, E., and Reijmer, C. H.: Reassessment of the Antarctic surface mass balance using calibrated output of a regional atmospheric climate model, J. Geophys. Res., 111, D11104, doi:10.1029/2005JD006495, 2006.
Vaughan, D. G., Bamber, J. L., Giovinetto, M., Russell, J., and Cooper, A. P. R.: Reassessment of net surface mass balance in Antarctica, J. Climate, 12, 933–946, 1999.
Warner, R. C. and Budd, W. F.: Derivation of ice thickness and bedrock topography in data-gap regions over Antarctica, Ann. Glaciol., 31, 191–197, 2000.
Zwally, H. J., Giovinetto, M. B., Li, J., Cornejo, H. G., Beckley, M. A., Brenner, A. C., Saba, J. L., and Donghui, Y.: Mass changes of the Greenland and Antarctic ice sheets and shelves and contributions to sea-level rise: 1992–2002, J.Glaciol., 51, 509–527, 2005.
Zwally, H. J., Schutz, B. E., Bentley, C. R., Bufton, J., Herring, T., Minster, J. F., Spinhirne, J., and Thomas, R.: GLAS/ICESat L2 Antarctic and Greenland Ice Sheet Altimetry Data V428, 25th September 2003 to 27th November 2006, Boulder, CO, National Snow and Ice Data Center, Digital Media, 2007.

Table 1. Operation periods of GLAS data used in current DEM.

Laser	Start Date	End Date
2a	25/09/2003	18/11/2003
2b	17/02/2004	21/03/2004
3a	03/10/2004	08/11/2004
3b	17/02/2005	24/03/2005
3d	21/10/2005	24/11/2005
3e	22/02/2006	27/03/2006
3g	25/10/2006	27/11/2006

Table 2. Amount of GLAS data removed by each stage of the QA filtering.

Filter	No of datapoints	Percentage remaining
Original data	76330444	
After geophysical filters	62844664	82.3%
After 3 sigma filter	62540388	81.9%
After DEM filter	59465625	77.9%

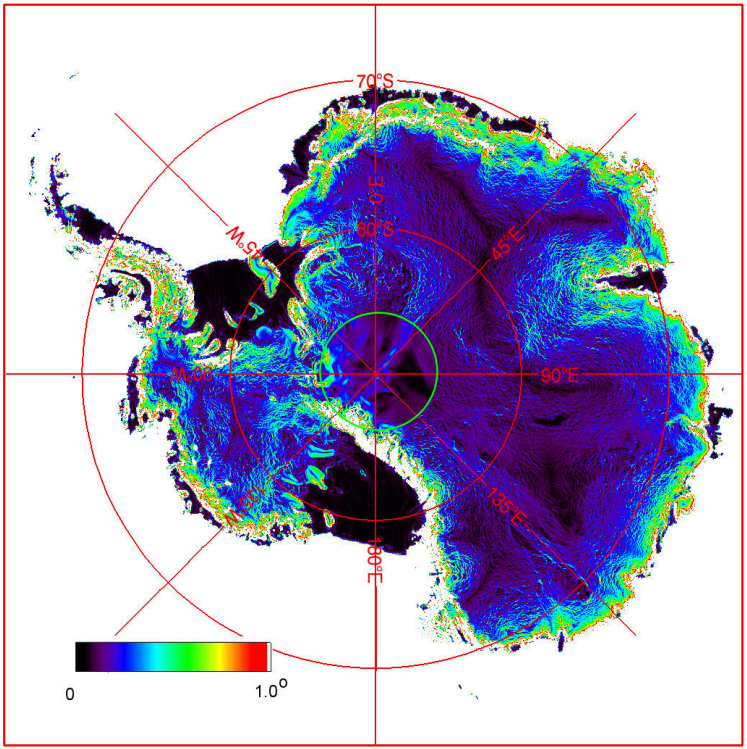

Fig. 1. Surface slopes, estimated from the new DEM over a 2 km length scale. The limit of satellite altimeter coverage is indicated by the green circle at 86° S.

TCD
2, 811–841, 2008

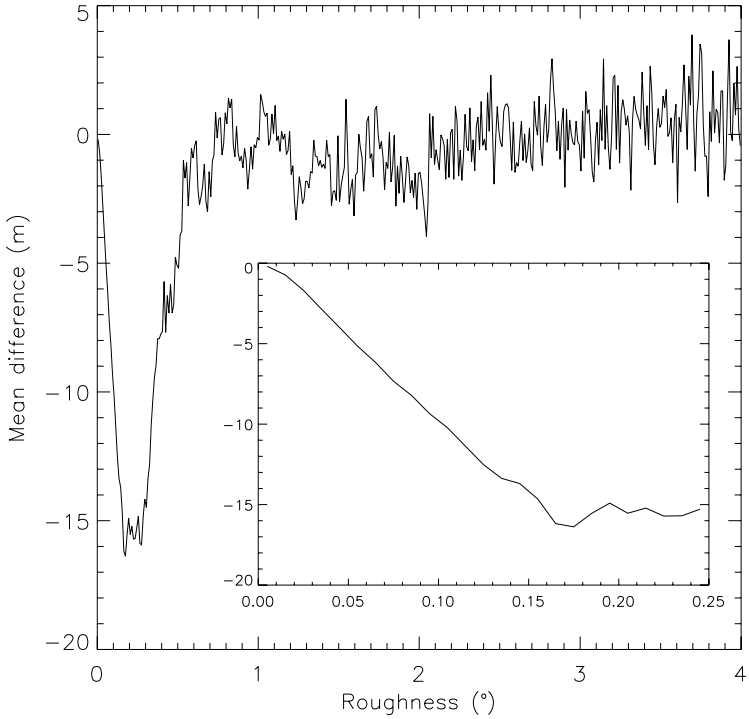

Fig. 2. Plot of the mean difference (GLAS-ERS-1) between the GLAS and ERS-1 data over Antarctica as a function of surface roughness. The inset shows the first part of the graph, up to 0.25°, for which a bias correction was applied.

TCD
2, 811–841, 2008

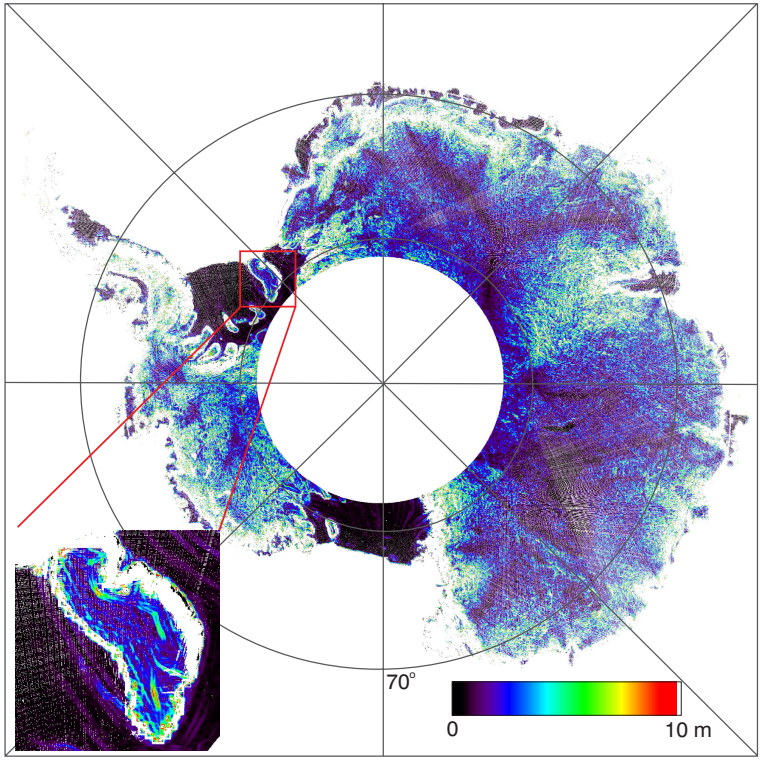

Fig. 3. Spatial distribution of the roughness-bias correction, between 0 and 10 m, applied to the ERS-1 data. The inset shows Berkner Island and surrounding shelf ice. The unshaded areas over the continent are mainly areas where no ERS-1 data were present.

TCD

2, 811–841, 2008

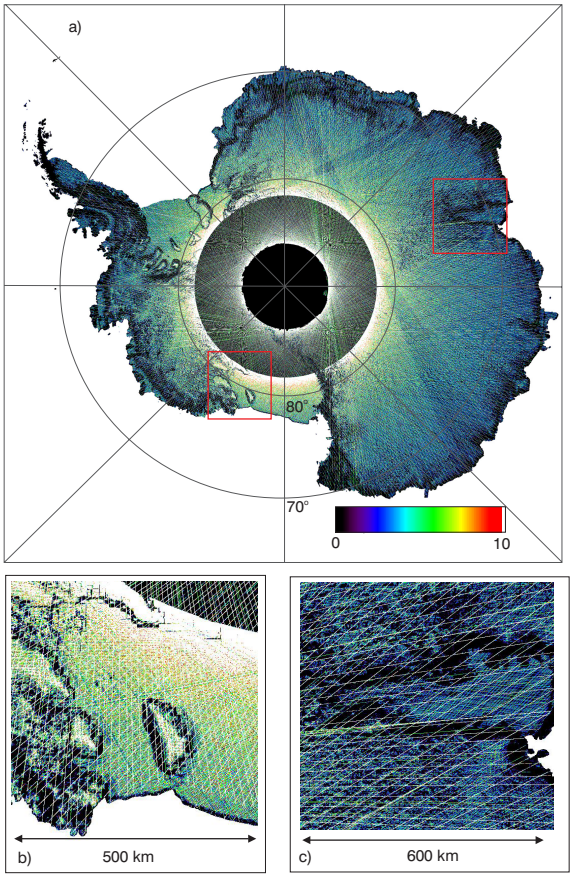

Fig. 4. Number of satellite observations between 0 and 10 in each 1 km grid cell. **(a)** covers the whole continent. The red boxes indicated the areas shown in (b) and (c). **(b)** shows a section of the Ross Ice Shelf including the Siple Coast and Roosevelt Island; **(c)** shows the Amery ice shelf and surrounding grounded ice sheet region.

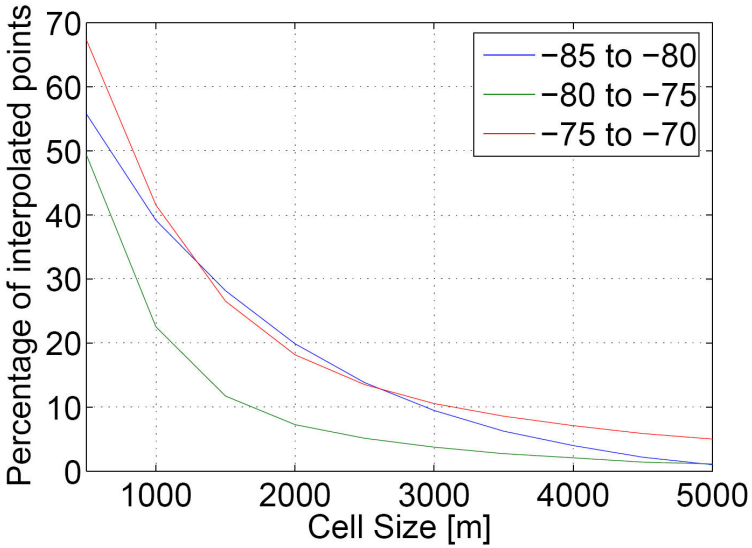

Fig. 5. Percentage of interpolated cells as a function of cell size and latitude for combined ERS and GLAS data.

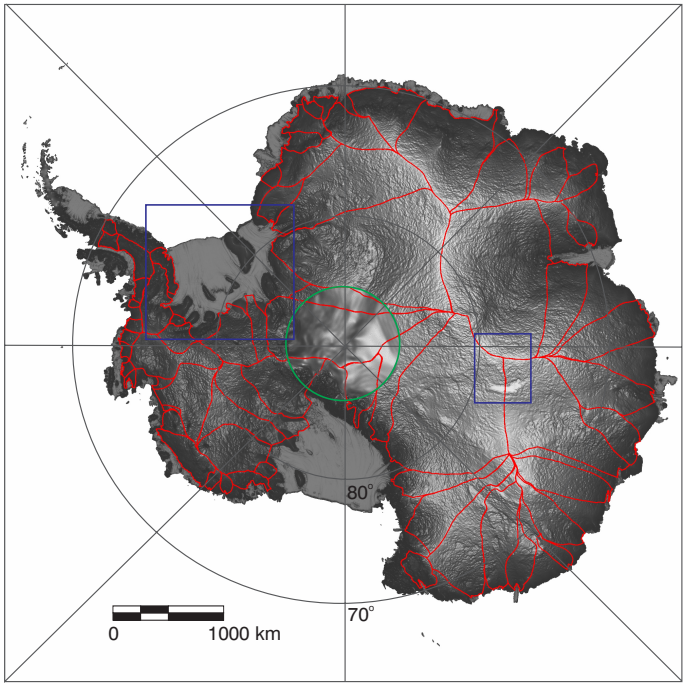

Fig. 6. Planimetric shaded relief plot of the 1 km digital elevation model. Ice divides, derived from the DEM, are shown in red; the green circle marks the limit of satellite altimeter coverage; the two blue boxes indicate the areas plotted in greater detail in Figs. 7 and 9.

TCD
2, 811–841, 2008

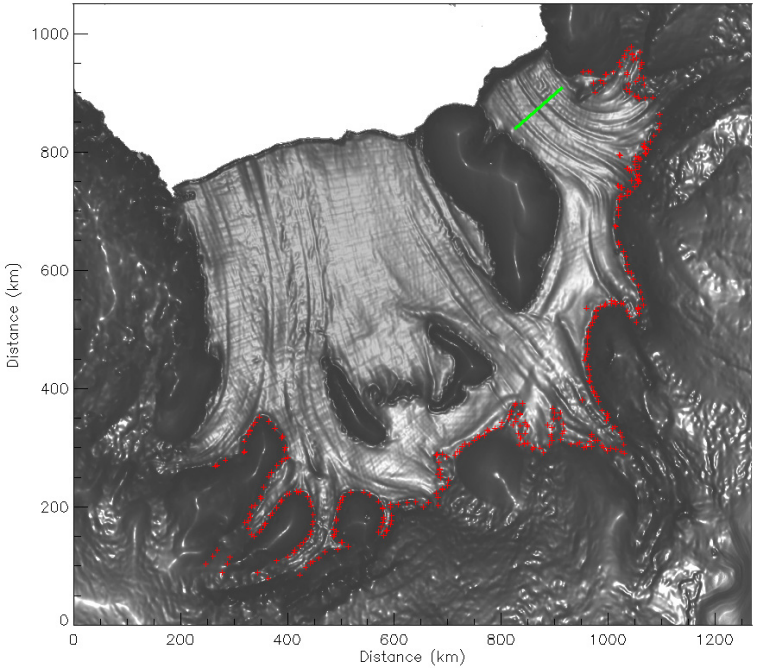

Fig. 7. Shaded relief plot of the Filchner Ronne Ice Shelf and surrounding grounded ice sheet. The red crosses indicate the location of the grounding zone identified using repeat-track analysis of GLAS data (Fricker and Padman, 2006). The green line shows the location of the elevation profile plotted in Fig. 8.

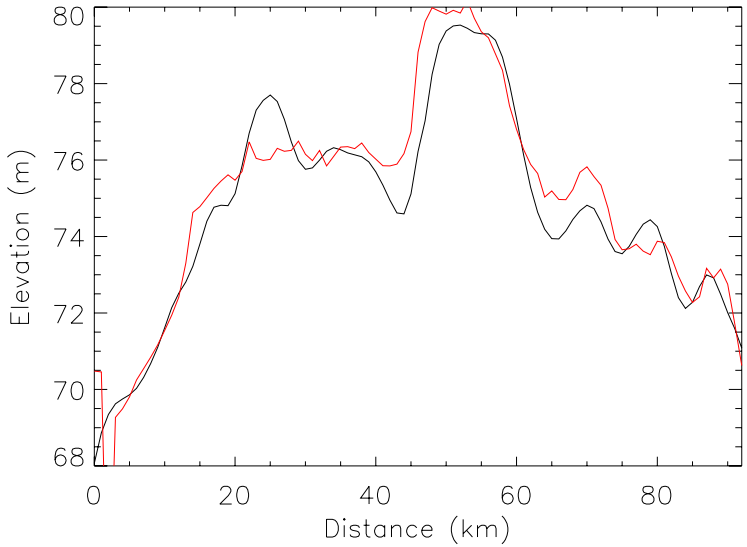

Fig. 8. Profile of elevation across the Filchner Ice Shelf indicating the amplitude and wavelength of "flow-stripes" associated with inflow of ice streams and glaciers feeding the ice shelf (c.f. Fig. 7 for location). Black line is for the DEM presented here, red line is for the ICESat DEM (DiMarzio et al., 2008).

TCD
2, 811–841, 2008

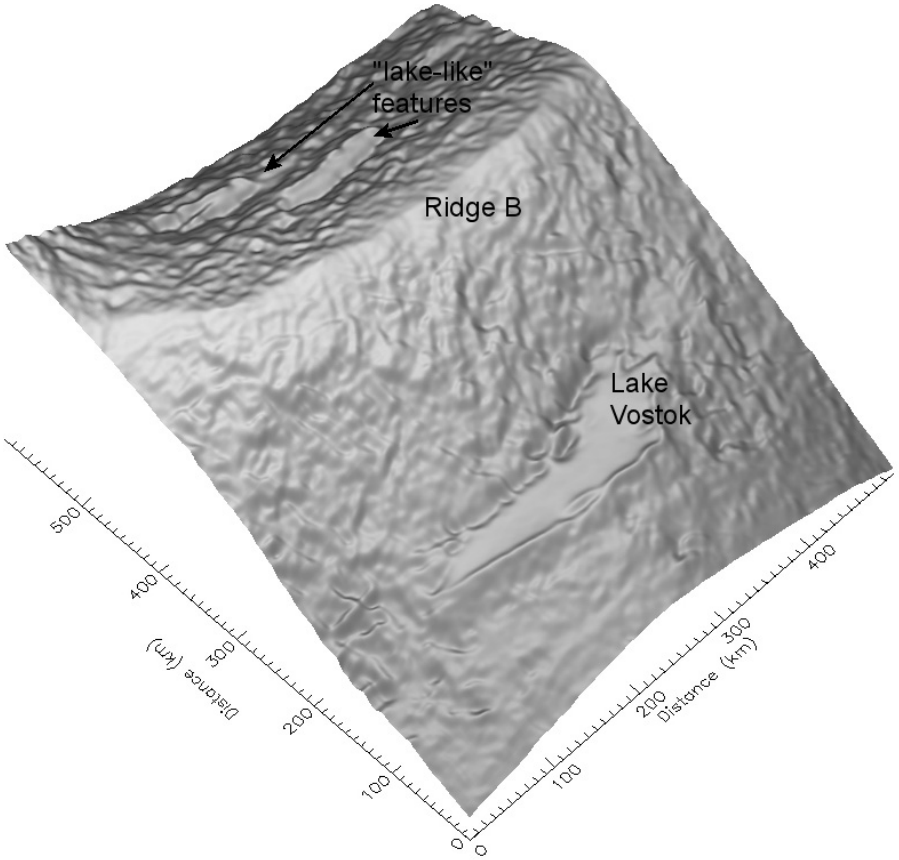

Fig. 9. Shaded relief plot using a perspective view covering the Lake Vostok-Ridge B region. The surface expression of two smaller "lake-like" features are visible on the other side of Ridge B.

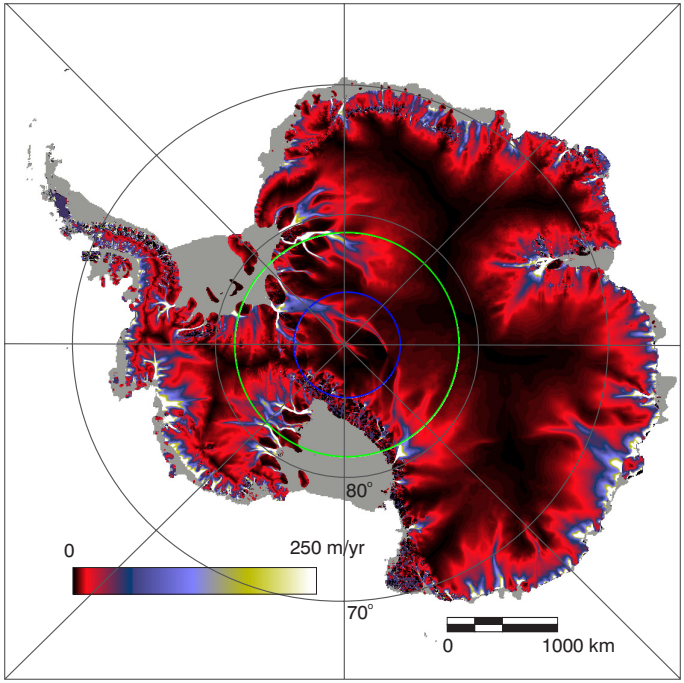

Fig. 10. Balance velocities for Antarctica, calculated at 5 km spacing using the new digital elevation model, accumulation rates from the output of a regional climate model (van de Berg et al., 2006) and the BEDMAP ice thickness compilation (Lythe and Vaughan, 2001) supplemented with new thickness data for the Amundsen Sea Sector (Holt et al., 2006). The green circle marks the limit of satellite altimeter data used in earlier DEMs of Antarctica. The blue circle marks the limit in this study.

TCD
2, 811–841, 2008

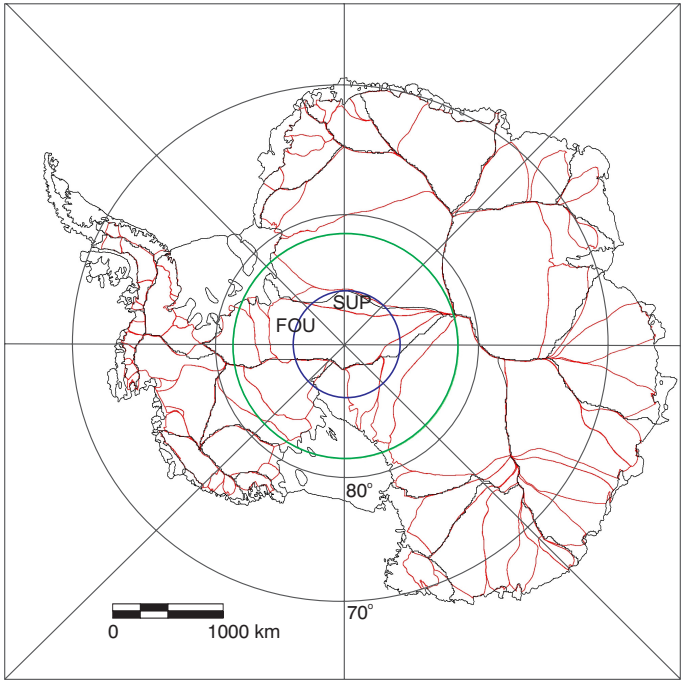

Fig. 11. Drainage basins estimated from an older radar altimeter DEM of Antarctica, in black, (Vaughan et al., 1999) compared with basins identified using the new 1 km DEM (Rignot et al., 2008) shown in red. The two coloured circles are as for Fig. 10. The catchments feeding Support Force and Foundation Ice Stream are indicated by SUP and FOU, respectively.

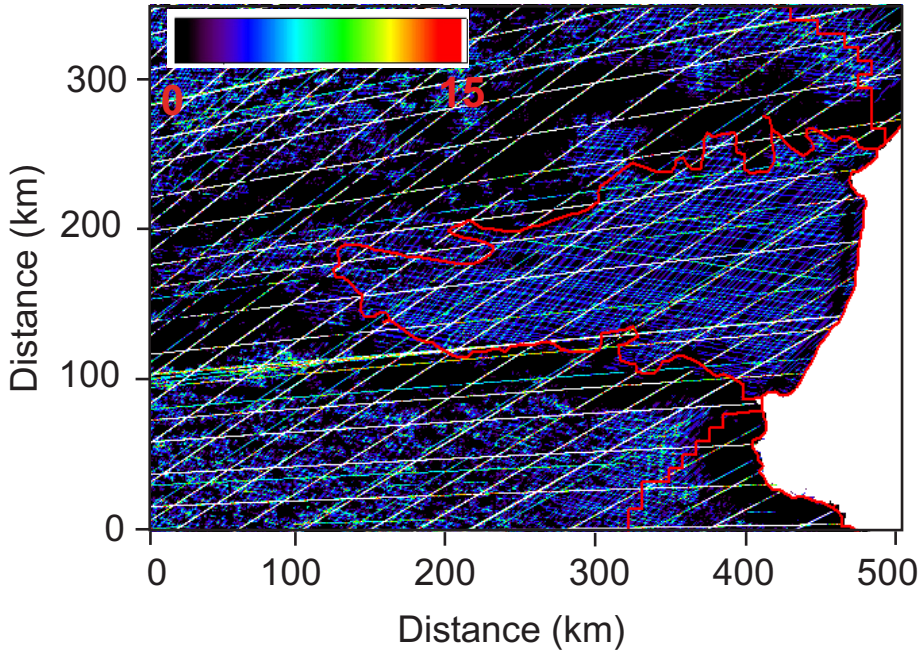

Fig. 12. Number of satellite observations between 0 and 15 in each 1 km grid cell for the Lambert Glacier region and Amery Ice Shelf. The grounding line for the ice shelf, from the Antarctic Digital Database, is shown in red.

TCD
2, 811–841, 2008